

# Autler-Townes splitting in two-color photoassociation of ${}^6\text{Li}$

U. Schlöder, T. Deuschle, C. Silber, and C. Zimmermann

*Physikalisches Institut, Eberhard Karls Universität,  
Auf der Morgenstelle 14, 72076 Tübingen, Germany*

(Dated: November 7, 2018)

We report on high-resolution two-color photoassociation spectroscopy in the triplet system of magneto-optically trapped  ${}^6\text{Li}$ . Photoassociation is induced from the ground-state asymptote to the  $v=59$  level of the excited  $1^3\Sigma_g^+$  state. This level is coupled to the  $v=9$  level of the triplet ground state  $a^3\Sigma_u^+$  by the light field of a Raman laser. The absolute transition frequencies are measured with an iodine frequency standard and the binding energy of the ground state is determined to  $24.391 \pm 0.020$  GHz. Strong coupling of the bound molecular states has been observed as Autler-Townes splitting in the photoassociation signal for different detunings of the Raman laser. From the splitting we determine the spontaneous bound-bound decay rate to  $4.3 \times 10^5 \text{ s}^{-1}$  and estimate the molecule formation rate. The observed lineshapes are in good agreement with the theoretical model.

PACS numbers: 32.80.Pj, 33.80.Ps, 34.20.Cf, 42.50.Hz

Coherent coupling schemes offer intriguing novel possibilities for the production of cold molecules. In such schemes, the continuum state of a free atom pair is coupled to a rovibrational level of the molecular ground state. Magnetic coupling in the vicinity of a Feshbach resonance has led to the observation of atom-molecule coherence in a  ${}^{85}\text{Rb}$  BEC [1] and to the selective production of weakly bound  $\text{Cs}_2$  dimers [2]. Optical coupling in stimulated Raman transitions has allowed for the creation of  ${}^{87}\text{Rb}$  molecules in a BEC [3] and of  $\text{Cs}_2$  molecules from a magneto-optically trapped atomic cloud [4]. In contrast to single-color photoassociation experiments, where cold ground-state molecules are produced incoherently by spontaneous decay of the optically excited dimer [5, 6, 7], these transition schemes have coherent character. Thereby, ground-state molecules are produced in a specific rovibrational level. In addition, the molecule formation rate can be strongly enhanced, as it is not limited by the small branching ratio between the bound-bound and the bound-free transitions. This is especially important for the formation of dimers with small intrinsic molecule formation rates, as in case of the absence of any favorable peculiarities in their potentials [5, 7]. While magnetic coupling schemes require a Feshbach resonance at sufficiently low magnetic fields and allow only for the production of cold molecules in weakly bound states, optical coupling schemes are more universal. Moreover, in extended multi-color versions, they are proposed for the production of molecules which are not only translationally, but also vibrationally cold [8].

Among the cold homonuclear dimers,  ${}^6\text{Li}_2$  molecules in the triplet state are particularly interesting. Combining two  ${}^6\text{Li}$  atoms to a  ${}^6\text{Li}_2$  molecule corresponds to transferring a Fermionic system into a Bosonic system. Such transition schemes are prerequisite for studying the ef-

fects of different quantum statistics on the reaction dynamics, the so-called superchemistry [9]. If, in addition, the molecule is prepared in the triplet state, it has a magnetic dipole moment. Storing these cold molecules in a magnetic trap should be possible, as demonstrated for cesium triplet dimers in a magnetic quadrupole trap recently [10].

In this paper we report on two-color photoassociation in the triplet system of  ${}^6\text{Li}_2$ . We use a Raman-type coupling scheme as shown in Fig. 1. Photoassociation is induced from the hyperfine ground-state asymptote  $f = 1/2 + f = 3/2$  into the excited triplet  $1^3\Sigma_g^+$  state by the photoassociation laser with frequency  $\nu_{\text{PA}}$ . From the excited rovibrational level  $v=59$ ,  $N=1$ , the specific hyperfine state |1111⟩ ( $|N S I G\rangle$ -notation, see e.g. [12])

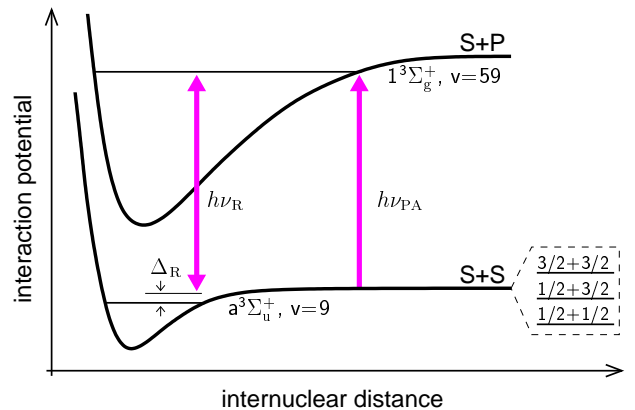


FIG. 1: Coupling scheme for the stimulated Raman photoassociation in the triplet system of the  ${}^6\text{Li}_2$  molecule. Photoassociation is induced from the ground-state asymptote  $1/2 + 3/2$  into the hyperfine state |1111⟩ of the excited level  $v=59$ . The Raman laser couples this excited level to the hyperfine state |0111⟩ of the ground-state vibrational level  $v=9$ .

is selected. The excited level lies at a laser detuning of  $-1787$  GHz relative to the  $D1$ -line, corresponding to a Condon point of about  $34 a_0$ . The natural linewidth is approximately twice the atomic value  $\Gamma$  and amounts to  $2\pi \times 11.7$  MHz [11]. The Raman laser of the frequency  $\nu_R$  couples the excited state to the hyperfine state  $|0111\rangle$  of the  $v=9$ ,  $N=0$  level of the triplet ground state  $a^3\Sigma_u^+$ . The ground-state level has a binding energy of approximately  $-24$  GHz and an outer turning point of  $27 a_0$ . The binding energies and the hyperfine structure involved in this scheme have been determined in photoassociation experiments of R. Hulet and co-workers [12, 13]. In our experiments we focus on an absolute frequency measurement of the bound-free and the bound-bound transition and therefore we deduce the binding energy of the ground state. Furthermore, we study the influence of the detuning of the fixed Raman laser on the photoassociation signal. Autler-Townes splitting in the two-color photoassociation signal is observed, which arises from the strong coupling of the bound molecular states. We discuss the lineshape in the light of the theory of Bohn and Julienne [14]. From the amount of the splitting we deduce the spontaneous decay rate and estimate the molecule formation rate. These results on the Autler-Townes splitting are complementary to recent two-color photoassociation experiments with cesium [4].

For the magneto-optical trap we use the two-species apparatus as described in [15], but operate it with  $^6\text{Li}$  only. We apply a detuning of  $-5\Gamma$  for the cooling transition and of  $-2\Gamma$  for the repumping transition. The temperature of the atomic ensemble can be estimated to  $0.5$  mK [16]. The particle number is monitored by absorption from a weak probe beam. For the photoassociation light we use a grating-stabilized diode laser with an output power of  $12$  mW. The light of the Raman beam is derived from a dye laser with  $500$  mW output power. The two laser beams are superimposed with parallel polarization and adjustable relative laser powers. The  $1/e^2$  diameters of the laser beams at the position of the atomic cloud amount to  $550 \mu\text{m}$ , corresponding to peak intensities of up to  $I_R = 40 \text{ W/cm}^2$  for the Raman laser and of up to  $I_{PA} = 7 \text{ W/cm}^2$  for the photoassociation laser. The stabilization and tuning of the diode laser is achieved by means of a stabilization chain. The diode is locked to a Fabry-Perot etalon with  $300$  MHz free spectral range. This etalon is stabilized relative to a second diode laser, which is again stabilized to a reference diode laser by a heterodyne technique. This reference laser is locked to an atomic lithium resonance by radio-frequency sideband spectroscopy in a lithium cell. Absolute frequency calibration is achieved by a Doppler-free iodine fluorescence spectroscopy with an accuracy of  $10$  MHz [17]. The scan rate is chosen to  $0.5$ - $1$  MHz/s for the absolute frequency measurements and to  $0.36$  MHz/s for the Autler-Townes measurements. This is slow as compared to the loading time of the trap of  $15$  s. Thereby a resolution of a few

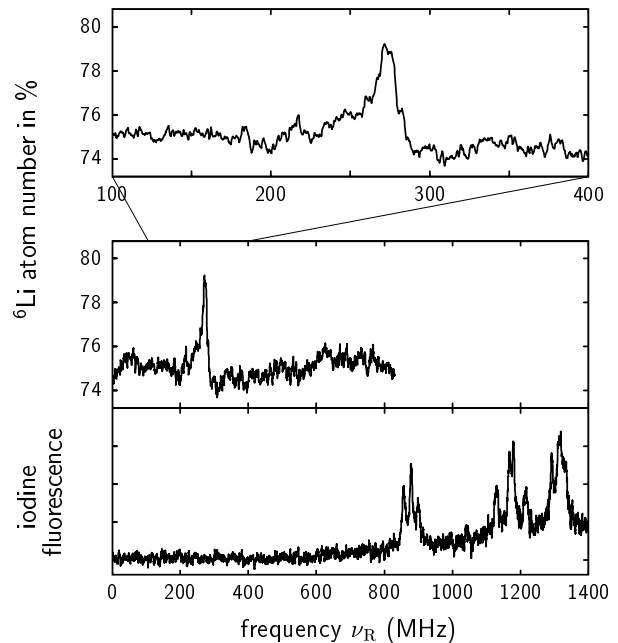


FIG. 2: Two-color photoassociation spectrum and iodine reference spectrum in the case of a fixed photoassociation laser and a scanned Raman laser. The offset to the axis of the Raman laser frequency  $\nu_R$  is  $445027$  GHz.

MHz is achieved.

For the absolute frequency measurement of the photoassociation and the Raman transition we proceed in the following manner. First, we record the single-color photoassociation spectrum and the iodine spectrum in the relevant frequency range simultaneously. For this special case we use the dye laser to induce photoassociation because of its larger tuning range. In order to keep the influence of the light shift [18] small, we reduce the laser intensity to  $3 \text{ W/cm}^2$ . For the transition from the hyperfine ground-state asymptote  $f = 1/2 + f = 3/2$  into the specific excited hyperfine state we determine the frequency to  $445002.881 \pm 0.015$  GHz. A redshift of  $10$  MHz due to the thermal energy of the atoms has been included in this analysis. Then, the photoassociation laser is held fixed on this transition, which leads to a decrease in the steady-state particle number of the trapped atoms to  $75\%$ . The Raman laser is scanned with an intensity of  $10 \text{ W/cm}^2$ . An increase in the particle number reveals resonance frequency of the Raman laser with the bound-bound transition, which lies at  $445027.272 \pm 0.013$  GHz (Fig. 2). At our relatively high Raman laser intensities, this reduction of decrease originates from the strong coupling of the bound molecular states by the Raman laser (see below), as a consequence of which the photoassociation laser is no longer resonant with the free-bound transition and particle losses due to photoassociation are suppressed. The binding energy of the bound ground-state

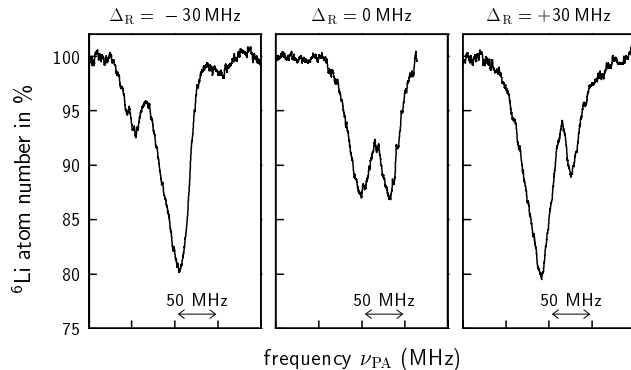


FIG. 3: Autler-Townes splitting for three different detunings  $\Delta_R$  of the Raman laser. The axis of the photoassociation laser frequency  $\nu_{PA}$  shows relative frequency calibration.

level  $v=9$  in the absence of hyperfine structure is equivalent to the difference between the measured transition frequencies, because the initial and final level are shifted due to the hyperfine structure by the same amount. We obtain a value of  $24.391 \pm 0.020$  GHz. The uncertainty is mainly due to a possible systematic error in the iodine reference spectrum and moreover due to the error in the determination of the line position. Our result is in agreement with the value of  $24.43 \pm 0.02$  GHz obtained from a direct measurement of the frequency difference [12].

The lineshape of the two-photon signal shows strong asymmetries with a shallow slope at the low frequency side and a steep slope at the high frequency side. We determine the linewidth (full width at half maximum) to 15 MHz. Therewith, the linewidth is smaller than the convolution of the natural linewidth of 11.7 MHz and the thermal broadening of about 10 MHz. The lineshape is that of a typical Fano profile [19, 20], which has been analyzed experimentally in [21].

For the Autler-Townes measurements, we first tune the Raman laser into resonance with the bound-bound transition for calibration. Then, a fixed detuning  $\Delta_R$  is added and the photoassociation laser is scanned. Two-color photoassociation spectra for three different detunings  $\Delta_R$  of the Raman laser are shown in Fig. 3. The spectrum in the middle has been taken in presence of a resonant Raman laser ( $\Delta_R = 0$  MHz). For the outer spectra, the Raman laser was detuned by the same amount of 30 MHz to the red and to the blue respectively. For these spectra, the laser intensities were chosen to  $30 \text{ W/cm}^2$  for the Raman laser and to  $3 \text{ W/cm}^2$  for the photoassociation laser. All three resonances show a doublet structure with a splitting of several 10 MHz. In the case of the resonant Raman laser, the resonance is split into two peaks with equal depth. For a detuned Raman laser, the splitting is asymmetric with a larger peak on the high-frequency side for red detuning and with a larger peak on the low-frequency side for blue detuning. To determine the split-

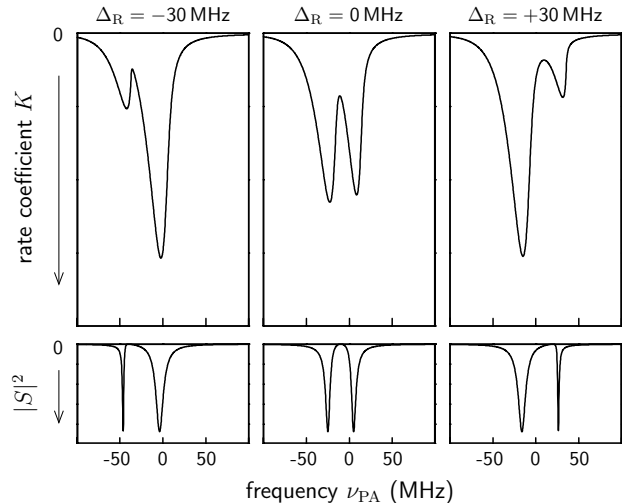


FIG. 4: Scattering probability  $|S|^2$  for a scattering energy of  $E/h = 10$  MHz and rate coefficient  $K$  for a temperature of 0.5 mK for three different detunings  $\Delta_R$  of the Raman laser. For the Rabi frequency  $\Omega = 2\pi \times 30$  MHz and for the natural linewidth  $\gamma = 12$  MHz were assumed. The frequency axis is relative to the transition frequency for vanishing energy. To compare the calculation with the experimental data, the ordinate is plotted upside-down.

ting we fit two Lorentzian functions to the data. For the resonant Raman laser the spacing between the maxima of the resonances amounts to 34.6 MHz. For the detuned Raman laser the spacing is 50.1 MHz and 40.4 MHz respectively.

The origin of the splitting can be explained in the dressed-state picture [20]. Here, the two bound molecular states are dressed with the light field of the Raman laser, forming a ladder of doublets that are separated by the generalized Rabi frequency  $\Omega_{\text{gen}}/2\pi$ . Its value depends on the detuning  $\Delta_R$  of the Raman laser and of the Rabi frequency  $\Omega$  (see below) according to  $\Omega_{\text{gen}}/2\pi = \sqrt{\Delta_R^2 + (\Omega/2\pi)^2}$ . By spectroscopy with a weak laser beam from a third level this splitting appears as an Autler-Townes doublet [22]. In the case considered here, this third level corresponds to the continuum state.

A more sophisticated model, also including lineshapes, is given by Bohn and Julienne [14]. This description is based on scattering theory and yields a general analytic expression for the two-color photoassociation scattering probability  $|S|^2$ . For a thermal ensemble, the corresponding rate coefficient  $K$  is obtained by thermal averaging. The results of a simulation for the corresponding parameters of our experiment are shown in Fig. 4. In this theory, the origin of the splitting is explained by two maxima of the scattering probability  $|S|^2$  as a function of the photoassociation laser frequency  $\nu_{PA}$ . The magnitude of the splitting is independent of the scattering energy  $E$  and corresponds to the generalized Rabi frequency  $\Omega_{\text{gen}}$ . By

thermal averaging over the scattering energies, the different resonance widths in the scattering probability  $|S|^2$  translate into different heights of the doublet peaks of the rate coefficient  $K$ . However, thermal averaging does not change the amount of the splitting substantially, which we have checked for various parameters. The thermal averaged resonances are asymmetric. The high-frequency sides are always steeper. This is due to the convolution of the small intrinsic linewidth of the transition with the Boltzmann distribution of the scattering energies  $E$ . Thereby, contributions from low energies, corresponding to higher frequencies, are favored.

The measured trap loss (Fig. 3) is proportional to the calculated photoassociation rate coefficient  $K$  (Fig. 4), if a linear response of the steady-state particle number to the rate coefficient  $K$  is assumed. For low photoassociation laser intensities this approximation is justified. The agreement concerning the splitting and the relative heights of the peaks between experiment and theory is quite good. Moreover, the asymmetry due to the thermal averaging is visible in the experimental spectra, particularly for the spectrum with  $\Delta_R = -30$  MHz.

For the experimental determination of the Rabi frequency  $\Omega$ , we use the data taken for a resonant Raman laser. In this case the generalized Rabi frequency  $\Omega_{\text{gen}}$  is identical to the Rabi frequency  $\Omega$  and independent of uncertainties in the detuning of the Raman laser. Therefore, the measured splitting of 34.6 MHz can be identified with the Rabi frequency  $\Omega/2\pi$ . By using the relation for the Rabi frequency  $\Omega = \sqrt{3c^2 I_R \Gamma_{\text{bb}} / 4\pi h \nu_R^3}$ , we determine the transition rate  $\Gamma_{\text{bb}}$  between the bound states to  $4.3 \times 10^5 \text{ s}^{-1}$ . This coincides well with a value of  $6.16 \times 10^5 \text{ s}^{-1}$  [8], derived theoretically from a simplified two-level system.

The experimental data allow an estimation of the molecular formation rate per atom and per second. For the resonant Raman laser, each doublet peak consists of contributions from the molecular ground state and from the excited state to equal parts. Thereby, the molecule formation rate should be given by half the single-color photoassociation rate. The photoassociation rate itself can be estimated from the 87% reduction of the steady-state number of  $^6\text{Li}$  atoms in presence of the photoassociation laser (see Fig. 3). Assuming constant density and using the measured value for the loading time of the trap, we use the formula given in [23]. We receive a value for the photoassociation rate in the range of  $0.01 \text{ s}^{-1}$  per atom, leading to a molecule formation rate in the same order of magnitude. This is an enhancement by a factor of 100 compared to the molecule formation rate due to single-color photoassociation, which can be estimated to  $8.4 \times 10^{-5} \text{ s}^{-1}$  by multiplying the photoassociation rate with the branching ratio between the bound-bound and the free-bound transitions [8]. For typical particle numbers in the order of  $10^8$  atoms [15], the absolute molecule formation rate amounts to  $10^6$  molecules/s. However, in

order to estimate the number of formed molecules, loss processes, such as spontaneous Raman scattering, have to be taken into account.

In conclusion, we have performed high-resolution two-color photoassociation spectroscopy in the triplet system of the  $^6\text{Li}_2$  molecule. The binding energy of the last bound level of the ground state has been determined in an absolute frequency measurement. We have observed the Autler-Townes splitting in the two-color photoassociation signal and therefrom deduced the bound-bound transition rate and the molecule formation rate. This rate is sufficiently high to encourage future experiments in this transition scheme. These are the accumulation of the cold triplet dimers in a magnetic trap and the production of vibrationally cold ground-state molecules via multi-color photoassociation schemes. For the degenerate regime, even pulsed schemes such as STIRAP [24] are discussed.

We would like to thank H. Schnatz and B. Bodermann from the PTB Braunschweig and E. Tiemann for valuable help with the iodine spectroscopy. This work has been partially funded by the Deutsche Forschungsgemeinschaft.

- 
- [1] E. A. Donley, N. R. Claussen, S. T. Thompson, and C. E. Wieman, *Nature* **417**, 529 (2002).
  - [2] C. Chin, A. J. Kerman, V. Vuletić, and S. Chu, *Phys. Rev. Lett.* **90**, 033201 (2003).
  - [3] R. Wynar, R. S. Freeland, D. J. Han, C. Ryu, and D. J. Heinzen, *Science* **287**, 1016 (2000).
  - [4] B. Laburthe Tolra, C. Drag, and P. Pillet, *Phys. Rev. A* **64**, 061401(R) (2001).
  - [5] A. Fioretti, D. Comparat, A. Crubellier, O. Dulieu, F. Masnou-Seeuws, and P. Pillet, *Phys. Rev. Lett.* **80**, 4402 (1998).
  - [6] A. N. Nikolov, E. E. Eyler, X. T. Wang, J. Li, H. Wang, W. C. Stwalley, and P. L. Gould, *Phys. Rev. Lett.* **82**, 703 (1999).
  - [7] C. Gabbanini, A. Fioretti, A. Lucchesini, S. Gozzini, and M. Mazzoni, *Phys. Rev. Lett.* **84**, 2814 (2000).
  - [8] R. Côté and A. Dalgarno, *J. Mol. Spec.* **195**, 236 (1999).
  - [9] D. J. Heinzen, R. Wynar, P. D. Drummond, and K. V. Kheruntsyan, *Phys. Rev. Lett.* **84**, 5029 (2000).
  - [10] N. Vanhaecke, W. de Souza Melo, B. Laburthe Tolra, D. Comparat, and P. Pillet, *Phys. Rev. Lett.* **89**, 063001 (2002).
  - [11] R. Côté and A. Dalgarno, *Phys. Rev. A* **58**, 498 (1998).
  - [12] E. R. I. Abraham, W. I. McAlexander, J. M. Gerton, R. G. Hulet, R. Côté, and A. Dalgarno, *Phys. Rev. A* **55**, R3299 (1997).
  - [13] E. R. I. Abraham, W. I. McAlexander, H. T. C. Stoof, and R. G. Hulet, *Phys. Rev. A* **53**, 3092 (1996).
  - [14] J. L. Bohn and P. S. Julienne, *Phys. Rev. A* **54**, R4637 (1996).
  - [15] U. Schlöder, C. Silber, and C. Zimmermann, *Appl. Phys. B* **73**, 801 (2001).
  - [16] U. Schünemann, H. Engler, M. Zielonkowski, M. Wei-

- demüller, and R. Grimm, *Opt. Commun.* **158**, 263 (1998).
- [17] C. Silber, T. Deuschle, U. Schlöder, S. Günther, and C. Zimmermann, in *Interactions in Ultracold Gases: From Atoms to Molecules*, (M. Weidemüller, C. Zimmermann (Eds.), Wiley-VCH, Weinheim, 2003).
- [18] J. L. Bohn and P. S. Julienne, *Phys. Rev. A* **60**, 414 (1999).
- [19] U. Fano, *Phys. Rev.* **124**, 1866 (1961).
- [20] C. Cohen-Tannoudji, J. Dupont-Roc, and G. Grynberg, *Atom-Photon Interactions*, (Wiley, New York, 1998).
- [21] C. Lisdar, N. Vanhaecke, D. Comparat, and P. Pillet, *Eur. Phys. J. D* **21**, 299 (2002).
- [22] S. H. Autler and C. H. Townes, *Phys. Rev.* **100**, 703 (1955).
- [23] U. Schlöder, C. Silber, T. Deuschle, and C. Zimmermann, *Phys. Rev. A* **66**, 061403(R) (2002).
- [24] A. Vardi, D. Abrashkevich, E. Frishman, and M. Shapiro, *J. Chem. Phys.* **107**, 6166 (1997).